OBSERVATIONS ON FLOW FIELD AROUND AN ABUTMENT IN A TWO-STAGE CHANNEL

SIOW-YONG LIM

Associate Professor, School of Civil and Environmental Engineering, Nanyang Technological University, 50 Nanyang Ave., Block N1, Singapore 639798

JOKO NUGROHO

Research Scholar, School of Civil and Environmental Engineering, Nanyang Technological University, 50 Nanyang Ave., Block N1, Singapore 639798

This paper presents results of 3-D flow distributions around an abutment located on the floodplain of a two-stage channel. The vertical wall abutment occupied one-fifth of the floodplain length and the flow depth ratio of floodplain to the main channel was 0.4. Measurements were done using a 3-D Acoustic Doppler Velocimeter (ADV) and a propeller current meter. The effects of the abutment on the flow distributions before and after scouring process were analyzed in term of the mean velocities, turbulent intensity, and turbulent kinetic energy. In the floodplain, strong secondary flow towards the main channel direction was observed for sections near the abutment site. The order of magnitude in the spanwise and vertical velocity components near the abutment tip was around 0.8 and 0.2 times that of the streamwise velocity at the approach section, respectively. The presence of the abutment increases the turbulent kinetic energy especially at the region close to abutment due to the vortices generated by the flow blockage and diversion. The results show that the measured bed shear stress amplification at the abutment tip was 3.7 times that of the approach section. The observations presented are useful in understanding what effect an abutment had on the scouring process on the floodplain.

1 Introduction

Flow and scouring around bridge support structures, i.e. pier and abutment, are important on-going research topics. The effect of pier on the flow and its implication on the scour had been studied extensively compare to that of abutment case. Further study on flow and scour around abutment is needed for the case of an abutment placed in a two-stage channel as this is often the case in natural channels.

Several results of studies on flow around abutment in rectangular channel have been published. Kwan and Melville (1994) measured the flow field in a local scour hole around bridge abutment using hydrogen-bubble technique. At the approach section, the flow was seen as one-dimensional and it started to develop a three-dimensional flow as it gets close to the abutment. The flow near the nose of the abutment was nearly uniform, which was also observed by Rajaratnam and Nwachukwu (1983). Molinas, Kheireldin and Wu (1998) investigated the shear stress amplification around a vertical wall abutment. They analyzed the shear stress at the nose of the abutment as the sum of shear stress amplification caused by contraction and the presence of the abutment structure. Ahmed and Rajaratnam (2000) observed flow around a wing-wall abutment in

rectangular channel and recognized a complex 3D skewed flow in the upstream and surrounding regions of the abutment. It was found that most of the accelerated flow was at the lower level, near the abutment nose, where maximum depth of a scour hole is usually found.

This paper presents results of study on flow and local scouring around abutment in a floodplain. This is in view of the fact that most natural rivers consist of a main channel and one or two floodplains. The objective of the paper is to give insight on the effect of the placement of an abutment in the floodplain on the flow distribution across the two-stage channel cross section. Observations on the three-dimensional flow field for the flat and scoured bed condition were done and some of the results, mainly from flat bed condition, are presented and discussed in this paper.

2 Experimental Setup and Measurement

The experiments were conducted in an asymmetrical two-stage channel at the hydraulics modelling laboratory of the School of CEE, NTU, Singapore. The channel was 19 m long and 1.6 m wide with a fixed longitudinal bed slope of 0.00116. It consists of a floodplain and a main channel of 1 m and 0.6 m wide, respectively. The bank height of the main channel is 0.15 m. The channel bed was made of stainless steel, while the side-walls were made of glass. Starting at 11 m downstream from the flume entrance, there was a sand recess of 2.5 m long. The discharge was measured using a magnetic flow meter installed in the supply pipeline and flow depths were measured using a depth gauge. A valve was installed in the supply line to control the discharge and the water level was controlled by a tailgate placed at the downstream end of the channel.

The vertical wall abutment model was placed in the sand recess section in the floodplain at a distance of 12 m from the channel entrance. It is shaped like a box and was made of perspex of 0.5 cm thick. The dimensions of the abutment were 5 cm wide, 20 cm long and 70 cm high. A section of 2 m long at the upstream of the sand recess was coated with uniform sand with d_{50} = 0.9 mm. In plane bed experiments, the sand recess was covered with a sand-coated aluminum plate.

The point velocity was measured mainly using a 3D down-looking ADV probe. The upper 5 cm of the flow depth was not in the range of measurement due to the ADV feature. A complete vertical distribution of the streamwise velocity component can be obtained using an 8 mm propeller-type current meter. Point velocity measurements were done at sections A (2 m upstream of the abutment), B (0.5 m upstream of the abutment), C (0.20 m upstream of the abutment), D (at the abutment site cross section), E (0.20 m downstream of the abutment), and F (0.50 m downstream of the abutment) (see also Fig. 1). The flow rate for this run was 70 l/s. The mean flow depths at the floodplain and the main channel were 0.108 and 0.258 m, respectively. The mean velocity at the floodplain and the main channel were 0.238 m/s and 0.285 m/s, respectively.

After the completion of the flow measurements for the plane bed condition, the same flow conditions were used for a test where bed scouring was allowed to occur until the

equilibrium scour depth was attained. The scouring process took 21 days to reach the equilibrium state and the scoure hole dimensions were 0.235 m deep and 0.60 m wide at the abutment site. Prior to the velocity measurements, the scoured bed was fixed by spraying sodium bicarbonate and sodium silicate over the surface. Benson et al (2001) evaluated the applicability and durability of these chemicals in stabilizing the surface of the loose bed material.

3 Results and Discussion

3.1. *Flow Field in x-y Plane*

Figure 1 presents the flow field at a horizontal plane, 0.5 cm above the floodplain bed or 15.5 cm above the main channel bed. At the approach section, velocity at the floodplain is lower than that at the main channel because the effect of the bed boundary was dominant. Near the abutment tip, the deflection angle close to the bed is larger compare to that of the higher level. Ahmed and Rajaratnam (2000) observed similar flow deflection behavior for a wing-wall abutment in a rectangular channel. The velocity vectors in the main channel are slightly affected by the abutment. This can be observed from the vertical distribution of velocity presented in Section 3.3.

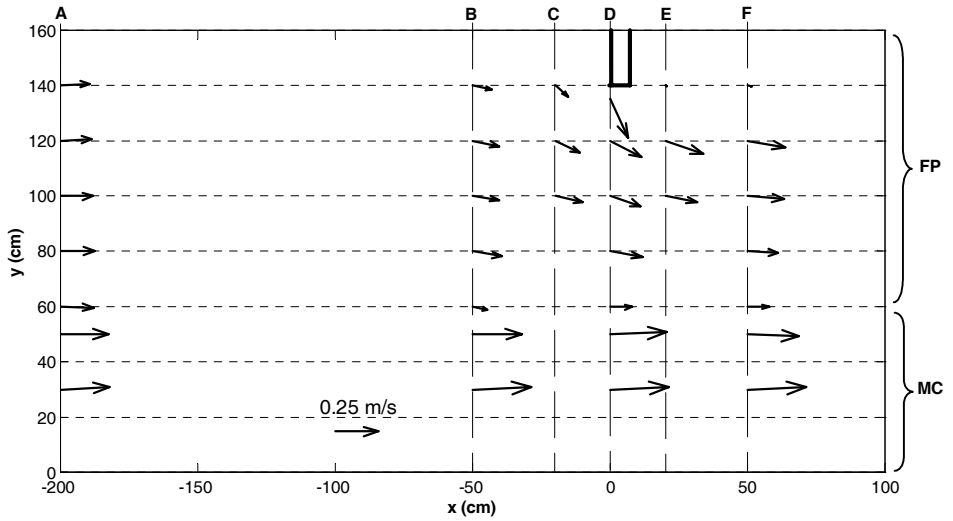

Figure 1. Velocity vectors at an *x-y* plane 0.5 cm above floodplain bed or 15.5 cm above main channel bed, under plane bed flow condition.

3.2. *Flow Field in y-z Plane*

Figures 2a and 2b show the velocity vectors in the *y-z* plane of section D for the plane bed condition and after the equilibrium scour hole was established, respectively. The

vectors are the resultant of *v* (spanwise) and *w* (vertical) velocity components. The velocity vectors of other sections for the plane bed conditions are not shown here but the essential features are also described together with that of section D.

In the plane bed condition, the spanwise velocity distributions for section A revealed that the flow was from the main channel towards the floodplain. As it passed through sections B to F, the flow direction reversed due to the blockage by the abutment. The largest magnitude of the spanwise and vertical velocities close to the abutment tip were around 0.8 and 0.2 times that of the mean streamwise velocity at the approach section (section A), respectively. The magnitude of secondary flow in the main channel at sections D and F increased considerably compared to that at section A. This is because the flow in the floodplain was diverted towards the main channel. At section D, near the abutment tip where the deepest scour depth occurred, the velocities at the lower depth were higher than those of the upper part. This is due to the effect of the flow diversion and the associated downflow at the abutment causing the flow velocity to be higher at the lower depth.

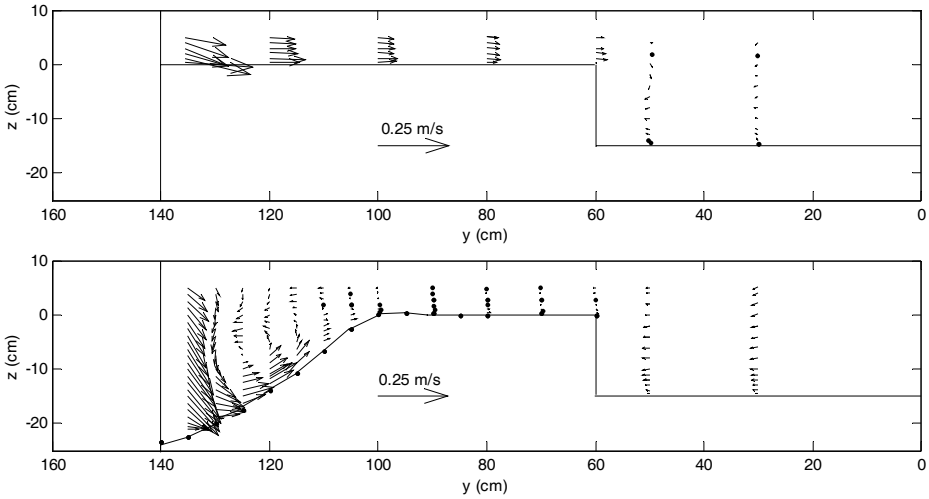

Figure 2. Secondary flow vectors at cross-section D at the plane bed (initial condition) and after the equilibrium scour hole was established.

After the scour hole was established, the overall spanwise velocity in the floodplain decreased. The flow pattern shows that at the mid and lower depth portion, an anticlockwise vortex was formed in the scour hole. A similar vortex was also observed by Kwan and Melville (1994) in their experiment for a wing-wall abutment placed in a rectangular channel. We observed that at section F this vortex was weak and there was another vortex with clockwise direction of rotation. At the downstream of the abutment, beside the streamwise sediment transport, the strong up-slopping flow transported the scoured sediment to the left and right side of the scour hole. The scoured sediments were deposited further downstream and also along the right and left edge of the scour hole.

The deposition along the sidewall at the area behind the abutment was higher compared to the opposite side.

3.3. *Vertical Distribution of Mean Velocity for Plane Bed Condition*

The vertical distributions of the streamwise (Fig. 3), spanwise (Fig. 4) and vertical (Fig. 5) velocity components are presented for two verticals, i.e. y = 100 cm in the floodplain and 30 cm in the main channel. The velocities were normalized using the overall mean velocity, U = 26.61 cm/s (total discharge divided by total flow area). For y = 80 to 140 cm in the floodplain, it was observed that the streamwise velocity decreases first and then increases as it passes section D. This can be seen in Figure 3a, for the case of y = 100 cm. The decrease in velocity was caused by the obstruction as the flow changes its direction and is diverted from the original streamwise direction. As it flows pass section D, the flow was deflected less and the increase in velocity was due to the flow area reduction. Figure 3b shows the change of streamwise velocity in the center line (y = 30 cm) of the main channel. It was observed that the streamwise velocity increases as it flows downstream.

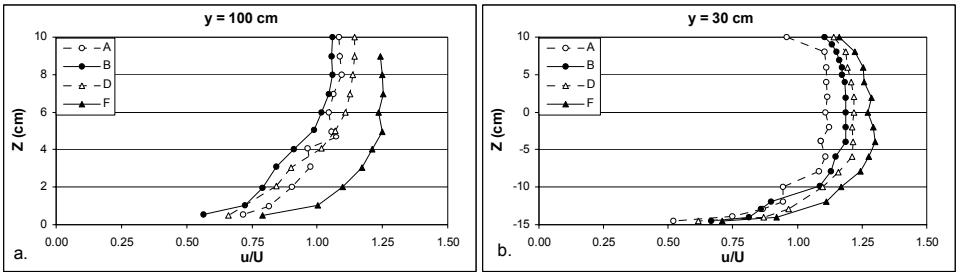

Figure 3. Streamwise velocity profiles at y = 100 cm (in the floodplain) and y = 30 cm (in the main channel).

Figure 4 shows the typical spanwise velocity distribution. In the floodplain for y between 80 to 140 cm, it was observed that the spanwise velocities at sections A, B and F were lower than that of section D. The change of velocity direction was also observed. Figure 4a shows that the spanwise velocity at y = 100 cm changes direction (negative v/U means flow towards the main channel) and has larger magnitude closer to the abutment. In the main channel, Figure 4b shows that the magnitude is decreasing for sections B and D, while for sections A and F there is not much different except for the lower part of the depth.

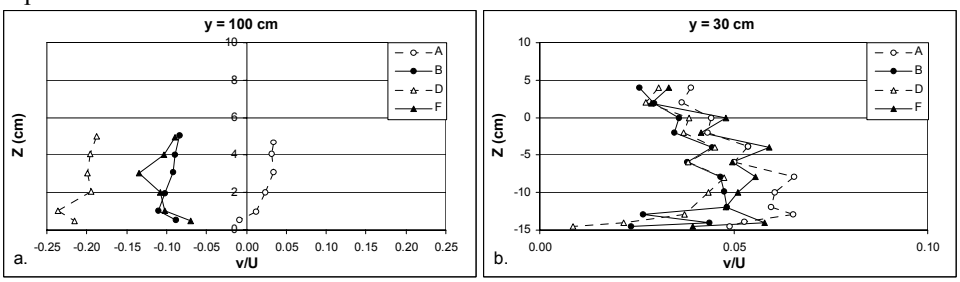

Figure 4. Spanwise velocity profiles at y = 100 cm (in the floodplain) and y = 30 cm (in the main channel).

Figure 5 shows the typical vertical velocity distribution. Significant changes of vertical velocity distribution were observed at the region near the abutment tip (sections B and D). In the main channel, the vertical velocity distribution at sections A, B, D and F has almost similar profile with increasing magnitude for the lower (positive w) and upper part (negative w).

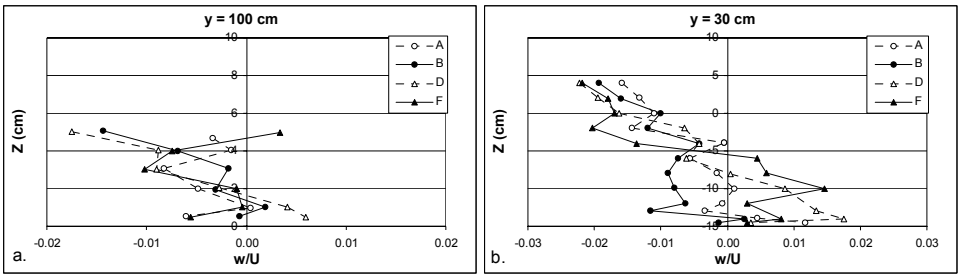

Figure 5. Vertical velocity profiles at y = 100 cm (in the floodplain) and y = 30 cm (in the main channel).

3.4. *Turbulent Intensity and Turbulent Kinetic Energy*

The normalized turbulent intensities are presented in terms of $u^+ = u'/U_*$, $v^+ = v'/U_*$ and $w^+ = w'/U_*$, where U_* = shear velocity at the floodplain approach section and u', v' and w' are the fluctuation of the streamwise, spanwise and vertical velocity components, respectively. The normalized turbulent intensity distributions of u^+, v^+ and w^+ at y = 120 cm (near the abutment) and 50 cm (near floodplain and main channel junction) are shown in Figures 6 to 8.

The effect of the abutment on the turbulent intensity on the floodplain was observed clearly along y = 140 and 120 cm. The magnitude of u^+, v^+ and w^+ along these transverse positions were increasing as it flows downstream, especially from sections D to F. In the middle of the main channel the distributions of turbulence intensities were similar for all observed cross sections. The changes were observed for y = 50 cm where u^+ and v^+ were increasing for the upper part and decreasing for the lower part, while w^+ was increasing only for the middle part. In general the magnitude of measured turbulent intensity shows that $u^+ > v^+ > w^+$.

The normalized turbulent kinetic energy is presented as $k^+=0.5\ (u'^2+ v'^2+ w'^2)/U_*^2$. In general, the total magnitude of turbulence increases around the abutment and at the floodplain and main channel junction. Figure 9 shows that an increase of k^+ on the floodplain was clearly observed for y = 120 cm at cross section F, while for other cross sections they were relatively small. The results show that the vertical distribution of k^+ in the centerline of the main channel at y = 30 cm was not affected by the presence of the abutment, but for y = 50 cm, i.e. close to the junction of the floodplain and main channel, there was an increase in k^+ for z = -5 to 2.5 cm.

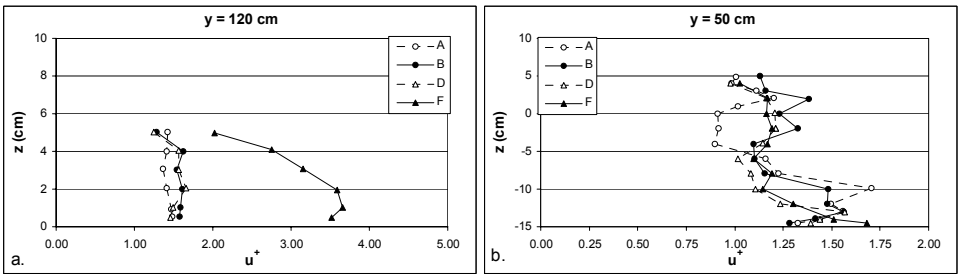

Figure 6. Streamwise turbulent intensity at y = 120 cm (in the floodplain) and y = 50 cm (in the main channel).

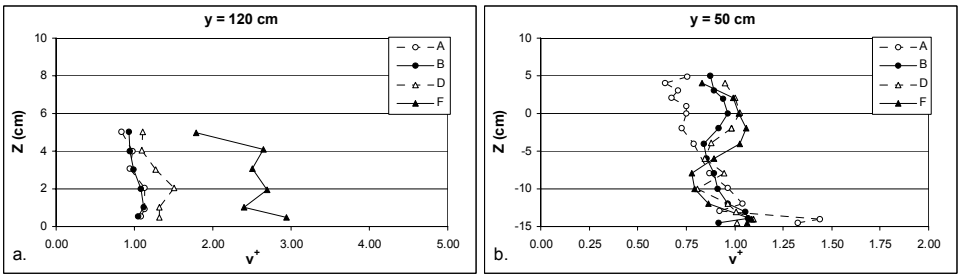

Figure 7. Spanwise turbulent intensity at y = 120 cm (in the floodplain) and y = 50 cm (in the main channel).

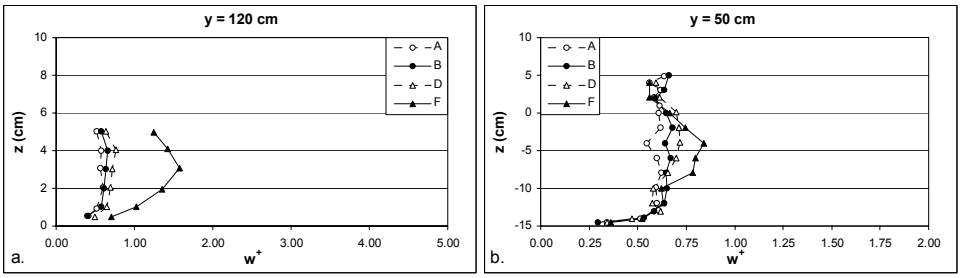

Figure 8. Vertical turbulent intensity at y = 120 cm (in the floodplain) and y = 50 cm (in the main channel).

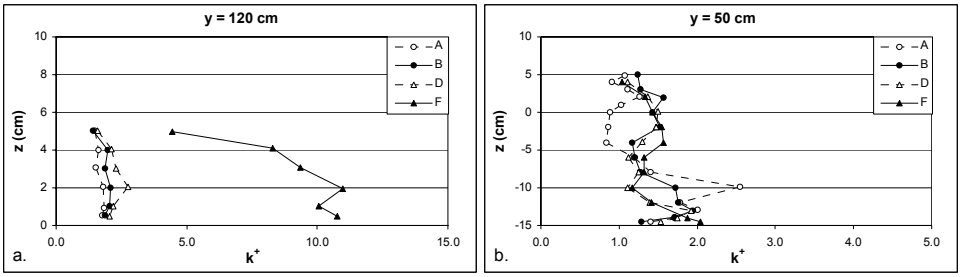

Figure 9. Turbulence kinetic energy at y = 120 cm (in the floodplain) and y = 50 cm (in the main channel).

3.5. *Bed Shear Stresses at Abutment Site*

The bed shear stresses were computed from the near bed velocity profile by assuming that log-law applies in this region. The bed shear stress obtained for a point close to the abutment tip was 3.7 times higher than that of the approach section or 1.8 times larger than the critical shear stress of the sediment used. The bed shear stress amplification is known to be the main cause of intense local scouring process around the abutment in conjunction with the transport due to the vortices system. Comparison between the computed streamwise bed shear stresses at the approach (section A) and abutment (section D) is presented in Figure 10.

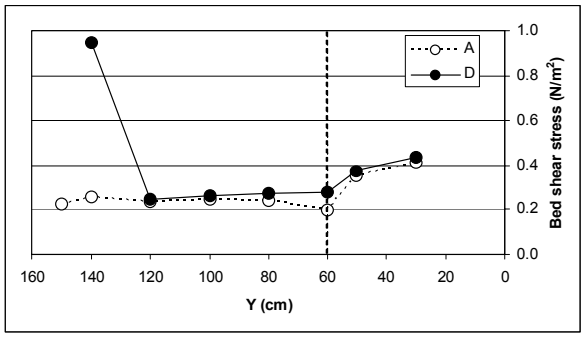

Figure 10. Bed shear stresses at cross sections A and D.

4 Conclusions

Observations on the flow around an abutment sited on the floodplain of a two-stage channel showed that the relatively short abutment affect significantly the velocity vectors for region close to the abutment. The streamwise velocity component accelerates as it flows pass the abutment site cross section. A small increase of the secondary flow magnitude was observed at the main channel, especially at cross section just downstream of the abutment. The spanwise velocity has a net flow direction from the floodplain towards the main channel for sections near the abutment, while the reverse is true for the approach cross-section.

The presence of the abutment increases the turbulent kinetic energy especially at the region close to the abutment due to the vortices generated by the flow blockage and diversion. The bed shear stress amplification for a point close to the abutment tip was 3.7 times larger than that of the approach section or 1.8 larger than the critical shear stress of the sediment used. In the scour hole, an anticlockwise vortex was formed at the section adjacent to the abutment. At the downstream of the abutment, this vortex was weakened and a clockwise vortex was formed behind the abutment.

Acknowledgments

The second writer acknowledges the financial support of Nanyang Technological University in the form of a research scholarship.

References

Ahmed, F. and Rajaratnam, N. (2000), "Observations on Flow Around Bridge Abutment", *Journal of Engineering Mechanics*, American Society of Civil Engineers, Vol. 126, No. 1, 51-59.

Benson, I.A., Valentine, E.M., Nalluri, C. and Bathurst, J.C. (2001), "Stabilising The Sediment Bed in Laboratory Flumes", *Journal of Hydraulic Research*, International Association of Hydraulic Engineering and Research, Vol. 39, No. 3, 279-282.

Kwan, R. T. F. and Melville, B. W. (1994), "Local Scour and Flow Measurement at Bridge Abutments", *Journal of Hydraulic Research*, International Association of Hydraulic Engineering and Research, Vol. 32, No. 5, 661-673.

Rajaratnam, N., and Nwachukwu, B. A. (1983), "Flow Near Groyne-Like Structures", *Journal of Hydraulic Engineering*, American Society of Civil Engineers, Vol. 109, No. 3, 463-480.

Molinas, A., Kheireldin, K., and Wu, B. (1998), "Shear Stress around Vertical Wall Abutments", *Journal of Hydraulic Engineering*, American Society of Civil Engineers, Vol. 124, No. 8, 822-830.